NFN - Nationales Forschungsnetzwerk

Geometry + Simulation

http://www.gs.jku.at

First order error correction for trimmed quadrature in isogeometric analysis

Felix Scholz and Angelos Mantzaflaris and Bert Jüttler

G+S Report No. 71

April 2018

Der Wissenschaftsfonds.

JOHANNES KEPLER UNIVERSITY LINZ

First order error correction for trimmed quadrature in isogeometric analysis

Felix Scholz, Angelos Mantzaflaris, and Bert Jüttler

Abstract In this work, we develop a specialized quadrature rule for trimmed domains, where the trimming curve is given implicitly by a real-valued function on the whole domain. We follow an error correction approach: In a first step, we obtain an adaptive subdivision of the domain in such a way that each cell falls in a predefined base case. We then extend the classical approach of linear approximation of the trimming curve by adding an error correction term based on a Taylor expansion of the blending between the linearized implicit trimming curve and the original one. This approach leads to an *accurate* method which improves the convergence the approximation error by one order. It is at the same time *efficient*, since essentially the computation of one extra one-dimensional integral on each trimmed cell is required. Finally, the method is *easy to implement*, since it only involves one additional line integral and refrains from any point inversion or optimization operations. The convergence is analyzed theoretically and numerical experiments confirm that the accuracy is improved without compromising the computational complexity.

1 Introduction

A common representation of a Computer-Aided Design (CAD) model is a boundary representation (B-rep), which typically consists of trimmed tensor-product NURBS patches. A trimmed surface patch consists of a tensor-product surface and a set of trimming curves on the surface that represent the boundary of the actual surface. Therefore, it represents only a part of the full tensor-product surface yet no explicit

Felix Scholz
Radon Institute for Computational and Applied Mathematics, Austrian Academy of Sciences, Linz, Austria, e-mail: felix.scholz@ricam.oeaw.ac.at

Angelos Mantzaflaris · Bert Jüttler
Institute of Applied Geometry, Johannes Kepler University Linz, Austria,
e-mail: angelos.mantzaflaris@jku.at, bert.juettler@jku.at

parametric representation is available. In this paper we are interested in applying numerical integration on a trimmed surface patch.

Computing integrals over trimmed domains both *efficiently* and *accurately* remains a challenging problem, notably for use in the frame of isogeometric analysis (IgA) [8]. The latter computational framework aims at a unification of the representations used in CAD and in numerical simulation, therefore operating directly on trimmed patches. The reader is referred to [15] for a recent review on trimming in CAD and IgA. We remark that different CAD representations are possible, e.g. subdivision surface-based models or T-spline models, see [1, 2, 9].

Multiple challenges arise for IgA on trimmed domains. One issue is the efficient coupling between adjacent trimmed patches. To this end, a finite cell method with weak coupling has been proposed in [19], a tearing and interconnecting approach was recently studied in [27] as well as Discontinuous Galerkin (DG) methods [6, 7, 26]. Another issue is the numerical stability of the trimmed basis functions, since basis functions with a tiny support can appear around the trimmed boundary. Several modified bases have been considered, such as immersed B-splines [20] and extended B-splines [14] to overcome the issue. Finally, the problem of applying numerical quadrature on a trimmed patch is a challenge in its own right.

One first approach to integrating over trimmed surfaces is to place quadrature points on the full surface and set the weights of the points lying outside the trimmed domain to zero. However, this method has no guarantees and the integration error cannot be controlled easily. In engineering practice local adaptive quadrature is used on top of it, that is, subdivision is performed around the trimmed region and quadrature nodes are placed in each sub-cell [5, 10, 23]. This approach can generate an extensive number of quadrature points, thus posing efficiency barriers.

Another approach is to perform a reparameterization (either globally, or locally at the element level), also known as “untrimming”; this puts more effort in the geometric side and results in tensor-product patches, which can be handled in an efficient way [22]. However, it is known that exact reparameterization is not feasible and approximate solutions result in cracks or overlaps in the model which require special treatment, e.g. by means of DG methods [6, 26]. In [11], the authors use base cases for the trimmed elements and perform local untrimming, using the intersection points of the trimmed curve and the boundary; see also [24] for some applications of this machinery in optimization. In [21] a local untrimming on the element level is performed by a projection method, which can be interpolation or least-squares fitting.

When the trimming curves are complicated and have high degree, it is typical to compute a piecewise linear approximation of the boundary to simplify further processing [1, 3, 12, 18]. However, when it comes to numerical integration, the geometry approximation error accumulates in the final result, and deteriorates the overall approximation order. Alternatively, in [16] the linearization is avoided, and a quadrature rule is constructed for each trimmed element by solving a moment-fitting, non-linear system to obtain quadrature nodes and weights, which are all contained inside the domain.

In the present work we develop an *efficient and accurate* quadrature rule for the approximation of integrals over trimmed domains. The trimming curve is given implicitly by a real-valued level function on the whole domain. This does not impose any restrictions, since any trimming curve can be converted into this format by employing implicitization techniques, which can be either exact or approximate ones, see, e.g., [4, 25]. Our method is based on an error correction approach. In a first step, we obtain an adaptive subdivision of the domain in such a way that each cell falls in a predefined base case. We then extend the classical approach of linear approximation of the trimming curve by adding an error correction term based on a Taylor expansion of the blending between the linearized implicit trimming curve and the original one.

In terms of *accuracy*, the method improves the local approximation error in each cell by two orders of magnitude compared to the piecewise linear approximation of the trimming curve, thus providing an extra order of convergence globally. In particular, cubic order of convergence is achieved with a negligible additional computational cost. The *efficiency* of the method is achieved by the fact that it requires solely the evaluation of the trimming function at the vertices of the cells and the quadrature nodes, and refrains from any kind of point inversion or non-linear solving. Furthermore, our method is *easy to implement*, since the resulting nodes for the correction term are simply one-dimensional Gauss nodes and their corresponding weights are given by a direct computation. Moreover, we do not need to test for quadrature points outside the integration domain or treat them in a different way. Overall, it is straight-forward to upgrade existing codes to incorporate our method.

In the next section, we state the problem of trimmed quadrature with a implicitly defined trimming curve. In Section 3 we explain the first step of the method, the subdivision of the domain into quadrature cells belonging to certain base cases. Section 4 deals with the piecewise linear approximation of the trimming function which is then extended by the first order error correction in Section 5. We analyze the convergence behavior of our method theoretically and experimentally in Sections 6 and 7, respectively.

2 Problem formulation

Throughout this paper, we consider integrals of bivariate functions on trimmed domains. More precisely, we assume that a sufficiently smooth function

$$f : [0,1]^2 \to \mathbb{R} \tag{1}$$

is given, which is defined on the entire unit square. In addition, we restrict the unit square by trimming with an implicitly defined curve $\tau(x,y) = 0$, which is defined by another smooth bivariate function

$$\tau : [0,1]^2 \to \mathbb{R}. \tag{2}$$

This results in the trimmed domain

$$\Omega_\tau = \{(x,y) \in [0,1]^2 : \tau(x,y) \geq 0\}. \tag{3}$$

We seek for quadrature rules that provide approximate values of the integral

$$I_\tau f = \int_{\Omega_\tau} f(x,y)\mathrm{d}y\mathrm{d}x. \tag{4}$$

These quadrature rules shall take the form

$$Q_\tau f = \sum_i w_i f(x_i, y_i) \tag{5}$$

with a finitely many quadrature nodes (x_i, y_i) and associated weights w_i. Two comments about this problem are in order:

1. As described in the introduction, this problem originates in isogeometric analysis, where one needs to solve it in order to perform isogeometric discretizations of partial differential equations on trimmed patches. Typically, the function f then takes the form

$$f(x,y) = DB_j(x,y)\bar{D}B_k(x,y)K(x,y) \tag{6}$$

   where the functions B_i are bivariate tensor-product B-splines or polynomial segments thereof and the kernel K reflects the influence of the geometry mapping (i.e., the parameterization of the computational domain by a NURBS surface) and the coefficient functions of the PDE. In many situations, this results in a piecewise rational function f.
2. Usually, the trimming functions in CAD and not given implicity but by low degree parametric curves. It is then possible to convert these curves into implicit form by invoking suitable implicitization techniques, which can be either exact or approximate ones, see e.g. [4, 25]

Our approach to finding a quadrature rule consists of two steps. First we subdivide the domain to reach a certain discretization size, while simultaneously ensuring that we arrive at a sufficiently simple configuration on each cell. Second we evaluate the contribution of each cell to the total value of the integral. These steps will be discussed in the next three sections.

3 Adaptive subdivision of the domain

Given a step size h, we subdivide the domain uniformly until the cell size does not exceed h. Subsequently, we perform adaptive subdivision until each resulting cell K is an instance of one of the five base cases depicted in Fig. 1. The resulting set of quadrature cells will be denoted by $\mathscr{K}$.

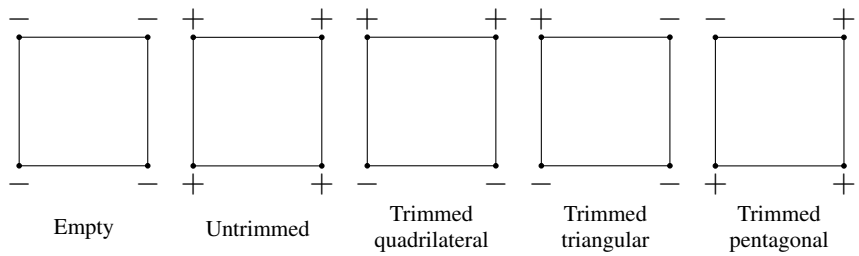

Fig. 1 Sign distributions of the trimming function τ for all five base cases (up to rotations).

More precisely, we use only evaluations of the trimming function at the cell vertices to identify the base cases, similar to the marching cubes algorithm [17]. Consequently, the method does not detect branches of the trimming curve that leave and re-enter the cell within the same edge. In order to illustrate this fact, Fig. 2 shows two instances of each trimmed base case.

Zero values at the vertices are treated as positive numbers. Consequently, there are only two sign distributions that do not represent a base case, see Fig. 3. These situations are dealt with by uniformly subdividing the corresponding cell. This process is guaranteed to terminate if no singularities of the trimming curve are present (which is always the case in practice).

We summarize our adaptive subdivision approach to the generation of quadrature cells $\mathscr{K}$ in the following algorithm.

- **QuadratureCells**, input: τ, $h > 0$
- Initialize the stack S by $[0,1]^2$.
- While $S \neq \emptyset$ do
  - $K = S.pop()$
  - if $Size(K) < h$ and $BaseCase(\tau, K)$
    Report K
    else
    $K_1, \ldots, K_4 = Quadsect(K)$
    $S.push(K_1, \ldots, K_4)$

Fig. 4 shows an instance of quadrature cells generated by the algorithm. The zero set of the trimming function consists of two parallel lines, which are parallel to one of the square's diagonals. The parameter h was chosen as $\frac{1}{2}$. For this specific instance of τ, the algorithm needs one or two additional subdivision steps at the northwest and southeast corners of the domain.

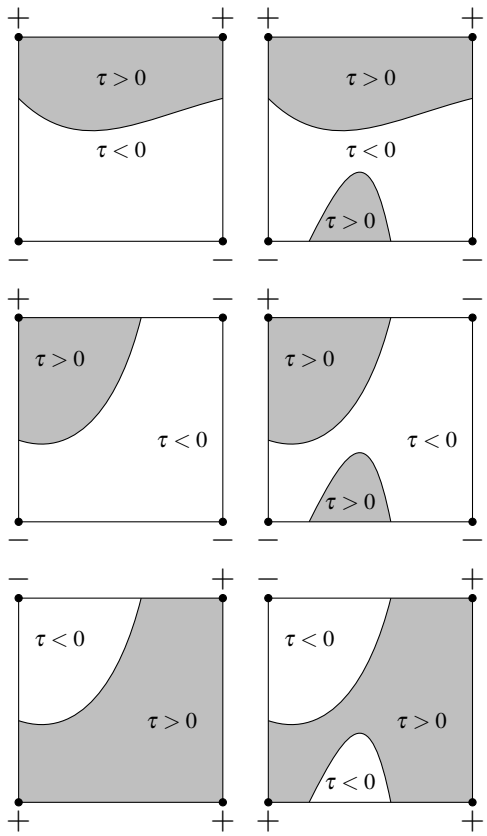

Fig. 2 Two instances of each trimmed base case (curved quadrilateral, triangle and pentagon).

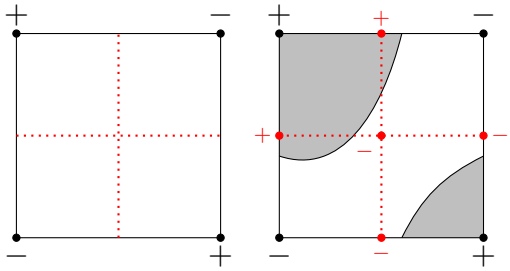

Fig. 3 Left: Sign distribution that does not represent a base case. Right: Uniform subdivision (quadsection) of this cell.

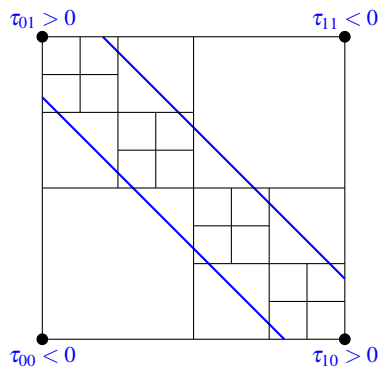

Fig. 4 Quadrature cells for $h = \frac{1}{2}$. The trimming curve is shown in blue.

4 Linearized trimmed quadrature

We perform the quadrature individually on each cell $K \in \mathscr{K}$. Thus, we need to approximate the integral

$$\int_{K_\tau} f(x,y)\mathrm{d}y\mathrm{d}x, \tag{7}$$

where

$$K_\tau = \{(x,y) \in K : \tau(x,y) > 0\}. \tag{8}$$

This approximation is trivial for the first two base cases: The value of the integral equals zero in the first case, and it is approximated by a tensor-product Gauss rule in the second one.

In order to perform this approximation in the remaining three base cases, we replace τ by another function σ. That function is chosen such that the integral

$$\int_{K_\sigma} f(x,y)\mathrm{d}y\mathrm{d}x \tag{9}$$

over the region

$$K_\sigma = \{(x,y) \in K : \sigma(x,y) > 0\} \tag{10}$$

enclosed by the zero-level set of σ admits a simple evaluation. This is achieved by using a linear approximation of τ. For this choice of σ, the level set $\sigma(x,y) = 0$ is simply a straight line segment.

The evaluation (9) by numerical quadrature is based on the intersections of $\sigma(x,y) = 0$ with the boundary of the cell. We determine these intersections by linear interpolation of the function values of τ at the vertices of the cell. This defines σ up to a scalar factor. Fig. 5 shows examples for this approximation. For this choice of σ, the linearized integral 9 belongs to the same base case as the original integral (7).

For the quadrilateral case we proceed as follows: First, we construct a bilinear parameterization of K_σ. Second, we transform the integral to the associated param-

eter domain and evaluate its value using Gauss quadrature with n evaluations per parametric direction, where n is chosen by the user. The triangular case is dealt with analogously, by using a parameterization with a singularity at the involved cell vertex. In the pentagonal case, the identity

$$K_\sigma = K \setminus K_{-\sigma} \tag{11}$$

allows to evaluate (9) by combining results for the untrimmed and the triangular case.

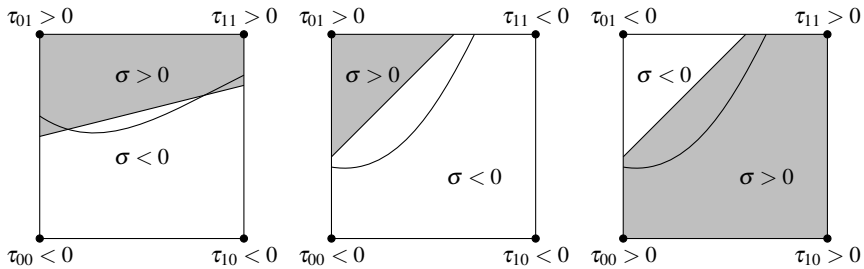

Fig. 5 A simple approximation of the three trimmed base cases.

The resulting linearized trimmed quadrature rule will be referred to as

$$\mathrm{LT}(h,n), \tag{12}$$

where h is the maximum cell size and n denotes the number of Gauss nodes. Clearly, the values generated by the LT rule converge to the true integral as h is decreased. As we shall see later, however, the rather rough approximation of the quadrature domain limits the order of convergence.

5 First order correction

We improve the order of convergence of the LT rule by adding an error correction term for the last three base cases. This term is found by performing a Taylor expansion.

Throughout this section, we consider a fixed trimmed cell

$$K = [x_0, x_0 + h] \times [y_0, y_0 + h] \in \mathscr{K} \tag{13}$$

which is either a quadrangular or triangular base case, see Figure 5. Recall that the pentagonal case is solved by considering the complementary triangular domain.

Linear blending of the trimming function τ and its linear approximation σ leads to the subsets

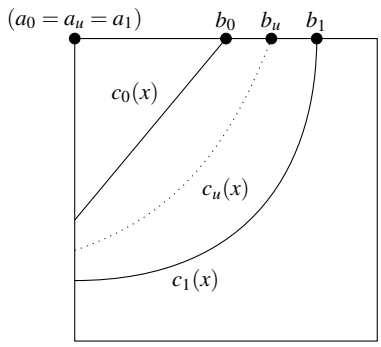

Fig. 6 Linear blending of τ and σ in the triangular base case.

$$K_{\sigma+u(\tau-\sigma)} = \{(x,y) \in K : \sigma(x,y) + u(\tau(x,y) - \sigma(x,y)) > 0\}, \quad u \in [0,1], \tag{14}$$

that define the function

$$F(u) = \int_{K_{\sigma+u(\tau-\sigma)}} f(x,y)\mathrm{d}y\mathrm{d}x. \tag{15}$$

It attains the exact value of (4) for $u = 1$, while the LT rule is based on the approximate evaluation of $F(0)$. We improve the accuracy by adding a correction term that is based on the first two terms of the Taylor series

$$F(1) = F(0) + F'(0) + R_1(1) \tag{16}$$

of F around $u = 0$, where R_1 denotes the remainder.

In order to compute $F'(0)$, we observe that the level set of the function obtained by linear blending defines a function $y = c_u(x)$ or $x = c_u(y)$ for sufficiently small values of u, where the projection of the trimming curve onto the x or y axis specifies the domain

$$[a_u, b_u], \tag{17}$$

respectively. If both choices are possible, we choose the one with the larger domain for $u = 0$.

Without loss of generality, we consider the first case

$$[a_u, b_u] \subset [x_0, x_0 + h] \tag{18}$$

where the function satisfies

$$\sigma(x, c_u(x)) + u(\tau(x, c_u(x)) - \sigma(x, (c_u(x)))) = 0, \tag{19}$$

see Figure 6. By differentiating (19) we observe that

$$\frac{\partial}{\partial u} c_u(x) = \frac{-\tau(x, c_u(x)) + \sigma(x, c_u(x))}{\frac{\partial \sigma}{\partial y}(x, c_u(x)) + u(\frac{\partial \tau}{\partial y}(x, c_u(x)) - \frac{\partial \sigma}{\partial y}(x, c_u(x)))}. \tag{20}$$

The function F in (15) can be rewritten as

$$F(u) = \int_{a_u}^{b_u} \int_{c_u(x)}^{y_0+h} f(x,y) \mathrm{d}y \mathrm{d}x. \tag{21}$$

Its first derivative thus evaluates to

$$\begin{aligned} F'(u) \;=\; & -\int_{a_u}^{b_u} f(x, c_u(x)) \frac{\partial}{\partial u} c_u(x) \mathrm{d}x \\ & -\frac{\mathrm{d}}{\mathrm{d}u} a_u \int_{c_u(a_u)}^{y_0+h} f(a_u, y) \mathrm{d}y + \frac{\mathrm{d}}{\mathrm{d}u} b_u \int_{c_u(b_u)}^{y_0+h} f(b_u, y) \mathrm{d}y \end{aligned} \tag{22}$$

The integration limit satisfies $b_u = x_0 + h$ or

$$c_u(b(u)) = y_0 + h. \tag{23}$$

Consequently, the third term in (22) vanishes since either the integral or the factor in front of it take value zero. Similarly, the second term vanishes as well.

Finally we use (20), (22) and the fact that σ vanishes on the graph of c_0,

$$\sigma(x, c_0(x)) = 0, \tag{24}$$

to rewrite the first order correction term

$$F'(0) = \frac{1}{\frac{\partial}{\partial y}\sigma} \int_{a_0}^{b_0} f(x, c_0(x)) \tau(x, c_0(x)) \mathrm{d}x \tag{25}$$

as a univariate integral over the linearized trimming curve. An approximate value is computed using a Gauss rule with k quadrature nodes.

The value of the correction term depends strongly on the choice of the derivative of the linearized trimming function, which we did not discuss so far. We use finite differences to derive the approximations

$$\frac{\partial \sigma}{\partial y} = \frac{\tau_{01} - \tau_{00} + \tau_{11} - \tau_{10}}{2h} \tag{26}$$

and

$$\frac{\partial \sigma}{\partial y} = \frac{\tau_{01} - \tau_{00}}{h} \tag{27}$$

which we employ in the quadrangular and triangular case, respectively.

The resulting corrected linearized trimmed quadrature rule (with first order correction term) will be referred to as

$$\mathrm{CLT}(h, n, k), \tag{28}$$

where h is the maximum cell size, and n resp. k are the numbers of bivariate resp. univariate quadrature nodes. In addition, we use

$$\mathrm{CLT}_K(h,n,k), \tag{29}$$

to denote the value contributed by an individual cell $K \in \mathscr{K}$.

If the trimming function τ is linear and thus $\sigma = \tau$, then

$$\tau(x, c_0(x)) = 0. \tag{30}$$

Consequently, the correction term (25) vanishes. In this case, CLT and LT give equivalent results.

6 Convergence result

In this section we will show that the first order error correction in the CLT rule improves the convergence by one order with respect to the non-corrected LT rule. More precisely, we will prove this result for a slightly modified version of CLT, obtained by adapting the quadrature cells, which we denote as $\mathrm{CLT}^\star$. The relationship between the original and the modified version will be revisited in Section 7.

First we prove two technical lemmas about the local errors in the trimmed cells of the quadrilateral base case (Lemma 1) and of the triangular base case (Lemma 2). Second we combine those local results with the known approximation properties of the employed Gauss rules to estimate the global approximation error in Theorem 1.

Both lemmas consider a cell $K = [x_0, x_0 + \alpha h] \times [y_0, y_0 + \beta h]$ and a trimming function τ defined on it. We consider the error of CLT_K as $h \to 0$. Moreover we assume that the cell satisfies the assumptions regarding the base cases in the strong sense, i.e., the trimming curve crosses the boundary in exactly two points.

Lemma 1. *Assume that K fulfills the assumptions of the quadrilateral base case in the strong sense, and the trimming function τ and its linear approximation σ satisfy the inequalities*

$$\left| \frac{\partial \tau}{\partial y}(x,y) \right| \geq C_1 \quad , \quad \forall (x,y) \in K \tag{31}$$

and

$$\|\sigma - \tau\|_{L^\infty(K)} \leq C_2 h^2, \tag{32}$$

$$\|\nabla\sigma - \nabla\tau\|_{L^\infty(K)} \leq C_3 h \tag{33}$$

for certain positive constants C_1, C_2, C_3. Then there exists a constant

$$C_{\mathrm{quad}}(C_1, C_2, C_3, f) \tag{34}$$

which depends solely on these three constants and f, such that the corrected trimmed quadrature on this cell fulfills for $n = k = 2$

$$|I_{\tau,K} f - \mathrm{CLT}_K(h,2,2) f| \leq C h^4. \tag{35}$$

Proof. Since by the monotonicity assumption (31) the trimming curve $\tau(x,y) = 0$ can be written as a graph, the same is true for all intermediate curves if h is sufficiently small. By differentiating (22) and using that both $a_u = x_0$ and $b_u = x_0 + \alpha h$ are constant, we obtain, for all $u \in [0,1]$,

$$F''(u) = -\int_{a_u}^{b_u} \frac{\partial}{\partial y} f(x, c_u(x)) \left(\frac{\partial}{\partial u} c_u(x) \right)^2 + f(x, c_u(x)) \frac{\partial^2}{\partial u^2} c_u(x) \mathrm{d}x \tag{36}$$

We observe that under the assumptions (31) - (33)

$$\left| \frac{\partial}{\partial u} c_u(x) \right| = \frac{|\tau(x, c_u(x)) - \sigma(x, c_u(x))|}{|(1-u)\frac{\partial}{\partial y}\sigma + u \frac{\partial}{\partial y}\tau(x, c_u(x))|} \leq C' h^2. \tag{37}$$

where C' depends on C_1, C_2, C_3. By differentiating (19) twice we obtain

$$\frac{\partial^2}{\partial u^2} c_u(x) = \frac{-2\frac{\partial}{\partial u} c_u \left(\frac{\partial}{\partial y}\tau - \frac{\partial}{\partial y}\sigma \right) - u \left(\frac{\partial}{\partial u} c_u \right)^2 \frac{\partial^2}{\partial y^2}\tau}{(1-u)\frac{\partial}{\partial y}\sigma + u \frac{\partial}{\partial y}\tau(x, c_u(x))} \tag{38}$$

and thus using again the assumptions on τ and σ we get

$$\left| \frac{\partial^2}{\partial u^2} c_u(x) \right| \leq C'' h^3 \tag{39}$$

where C'' depends again on C_1, C_2, C_3. By estimating the integral by the supremum we conclude that for all $u \in [0,1]$

$$F''(u) \leq C''' h^4. \tag{40}$$

The result is obtained by combining Taylor's theorem with the approximation properties of the employed Gauss rules for the bi- and univariate quadrature. □

Lemma 2. *Assume that K satisfies the assumptions of the triangular base case (in the strong sense) and that in addition to the assumptions (31)-(33) in Lemma 1 there is a constant C_4 independent of h, such that*

$$\left| \frac{\partial \tau}{\partial x}(x,y) \right| \geq C_4 > 0 \quad , \quad \forall (x,y) \in K \tag{41}$$

Then, there exists a constant $C_{\text{triangle}}(C_1, C_2, C_3, C_4, f)$, such that the corrected trimmed quadrature on this cell fulfills

$$|I_{\tau,K} f - \mathrm{CLT}_K(h,2,2) f| \leq C_{\text{triangle}} h^4. \tag{42}$$

Proof. In the triangular case, b_u in (22) is not constant but defined implicitly by

$$c_u(b_u) = y_0 + \beta h. \tag{43}$$

For the second derivative of F this means that an additional term appears which depends on the derivative of b_u:

$$\begin{aligned} F''(u) \;=\; & -\int_{a_u}^{b_u} \frac{\partial}{\partial y} f(x, c_u(x)) \left(\frac{\partial}{\partial u} c_u(x) \right)^2 + f(x, c_u(x)) \frac{\partial^2}{\partial u^2} c_u(x) \mathrm{d}x \\ & - f(b_u, c_u(b_u)) \frac{\partial}{\partial u} c_u(b_u) \frac{\mathrm{d}}{\mathrm{d}u} b_u. \end{aligned} \tag{44}$$

In order to estimate the last term in (44), we compute

$$\frac{\mathrm{d}}{\mathrm{d}u} b_u = -\frac{\frac{\partial}{\partial u} c_u(b_u)}{\frac{\partial}{\partial x} c_u(b_u)}. \tag{45}$$

Differentiating (19) with respect to x leads to

$$\frac{\partial}{\partial x} c_u(x) = -\frac{\frac{\partial}{\partial x}\sigma + u\left(\frac{\partial}{\partial x}\tau(x, c_u(x)) - \frac{\partial}{\partial x}\sigma\right)}{\frac{\partial}{\partial y}\sigma + u\left(\frac{\partial}{\partial y}\tau(x, c_u(x)) - \frac{\partial}{\partial y}\sigma\right)}. \tag{46}$$

Using assumption (41) we conclude

$$\left| \frac{\partial}{\partial x} c_u(x) \right| \geq C'''' > 0 \tag{47}$$

and thus

$$\left| \frac{\mathrm{d}}{\mathrm{d}u} b_u \right| \leq C''''' h^2. \tag{48}$$

Therefore, in view of (37) and (39) the last term in (36) satisfies

$$f(b_u, c_u(b_u)) \frac{\partial}{\partial u} c_u(b_u) \frac{\mathrm{d}}{\mathrm{d}u} b_u \leq C'''''' h^4 \tag{49}$$

and the result follows. □

For the analysis, we construct a modified quadrature rule CLT* by replacing the subdivision $\mathscr{K}$ of Ω with a new subdivision $\mathscr{K}^\star$. We begin by using the subdivision algorithm stated in Section 3 with a step-size of at most $\frac{h}{2}$. If h is small enough, then all resulting quadrature cells in $\mathscr{K}$ are squares of size $\frac{h}{2}$. We will obtain $\mathscr{K}^\star$ by merging some of the trimmed cells in $\mathscr{K}$.

First, we define the constants C_1 and C_4 that are to be used in Lemmas 1 and 2 as

$$C_1 = C_4 = \frac{1}{4} \min_{\tau(x,y)=0} \|\nabla \tau(x,y)\|_2. \tag{50}$$

If h is sufficiently small this means that each trimmed cell $K \in \mathscr{K}_{\text{trimmed}}$ is in one of three classes:

1. Class H (horizontal gradient): In K we have

$$\left|\frac{\partial}{\partial x}\tau(x,y)\right| \geq C_4, \text{ and } \left|\frac{\partial}{\partial y}\tau(x_0,y_0)\right| < C_1 \text{ for at least one } (x_0,y_0) \in K. \quad (51)$$

2. Class V (vertical gradient): In K we have

$$\left|\frac{\partial}{\partial y}\tau(x,y)\right| \geq C_1, \text{ and } \left|\frac{\partial}{\partial x}\tau(x_0,y_0)\right| < C_4 \text{ for at least one } (x_0,y_0) \in K. \quad (52)$$

3. Class D (diagonal gradient): In K we have

$$\left|\frac{\partial}{\partial x}\tau(x,y)\right| \geq C_4 \text{ and } \left|\frac{\partial}{\partial y}\tau(x,y)\right| \geq C_1. \quad (53)$$

This is illustrated in Fig. 7. If a cell K belongs to class H (resp. class V), then also all

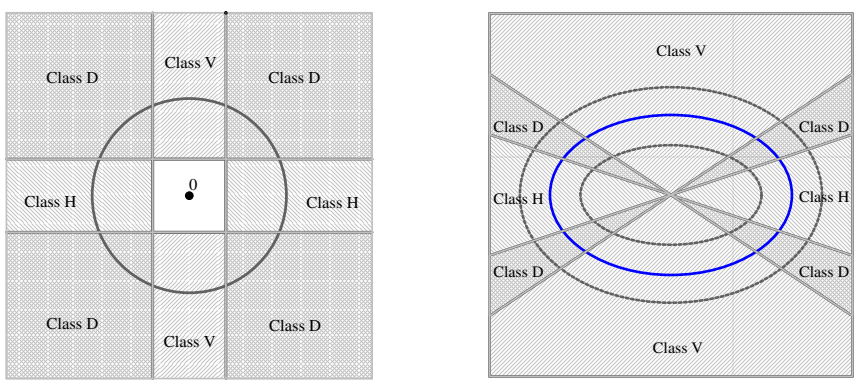

Fig. 7 Illustration of the regions of cell classes V, H and D. Left: The regions defined by $\nabla\tau(x,y)$ for (x,y) over the union of the trimmed cells. The black circle has radius $4C_1 = \min_{\tau(x,y)=0} \|\nabla\tau(x,y)\|_2$. It is visible that $\nabla\tau(x,y)$ lies outside the square in the middle. Right: An example trimming curve (an ellipse, shown in blue). The dotted offsets enclose the region that contains trimmed cells.

of its neighbors are either in class H (resp. V) or in class D. To obtain the modified subdivision $K^\star$ we merge all pairs of vertically adjacent cells where one of them is in class H. Similarly, we merge all pairs of horizontally adjacent cells where one of them is in class V. The remaining cells are kept. Note that this results in rectangular cells of maximum size h, since at most two cells will be merged, due to the restricted range of the gradients.

The modified rule CLT* is obtained by applying CLT to the modified subdivision $\mathscr{K}^\star$.

Next, we prove the convergence result for the modified rule CLT*.

Theorem 1. *Assume $\tau \in C^2([0,1]^2)$ such that the constant $C_1 = C_4$ as defined in (50) is positive, and $f \in C^4([0,1]^2)$. Then, there exists a constant $C_{\tau,f}$, such that the* CLT* *rule with $n = 2$ and $k = 2$ satisfies*

$$|I_\tau f - \mathrm{CLT}^\star(h,2,2)f| \leq C_{\tau,f} h^3. \tag{54}$$

Proof. By the construction of CLT*, the subdivision $\mathscr{K}^\star$ consists of untrimmed quadrature cells, trimmed quadrilateral cells of classes H, V and D, and trimmed triangular and pentagonal cells of class D. In the trimmed quadrilateral cells we can always apply Lemma 1, while in the trimmed triangular cells of class D we can apply Lemma 2. Moreover, we can treat the trimmed pentagonal cells of class D by applying Lemma 2 to the complement of the quadrature domain. In both cases the constants C_2 and C_3 are obtained by linear approximation of τ. They depend on the second derivative of τ whose norm is bounded.

The number of trimmed cells does not exceed $C_5 \frac{1}{h}$ for some constant C_5. Moreover, we can use the same constants C_{quad} and C_{triangle} for all trimmed cells. Indeed, these constants depend on the same values $C_1, \ldots, C_4$, and may use an upper bound on the derivatives of f. We conclude

$$\sum_{K \in \mathscr{K}^\star_{\mathrm{trimmed}}} |I_{\tau,K} f - \mathrm{CLT}_K(h,2,2)f| \leq C_5 \max\{C_{\mathrm{quad}}, C_{\mathrm{triangle}}\} h^3. \tag{55}$$

Since we use $n = 2$ Gauss nodes in each direction for the untrimmed cells, the local error is bounded by $C_{\mathrm{Gauss}} h^5$ in each of these cells for some constant C_{Gauss}. Since there are at most $\frac{1}{h^2}$ untrimmed cells, we have

$$\sum_{K \in \mathscr{K}^\star_{\mathrm{untrimmed}}} |I_{\tau,K} f - \mathrm{CLT}_K(h,2,2)f| \leq C_{\mathrm{Gauss}} h^3. \tag{56}$$

The result (54) is implied by these two inequalities, since the various constants depend on τ and f only. □

We conjecture that in the triangular base case the influence of the last term in (44) is canceled by the corresponding term in the adjacent cell. Consequently, in practice it suffices to use CLT instead of CLT*. This is supported by our numerical experiments, where CLT is tested.

7 Numerical experiments

We implemented the method in C++ using the G+Smo library [13]. In this section, we will test the approximation properties of the linearized trimmed quadrature rule CLT as well as the linearized trimmed quadrature rule LT on a number of trimmed

geometries. In the numerical experiments we observe that the theoretical error estimate for CLT* (Theorem 1) still holds for the CLT quadrature rule.

7.1 Ellipse

As a first example, we use our method to compute the volume of an ellipse implicitly defined by

$$\tau(x,y) = -\frac{(x-0.5)^2}{a^2} - \frac{(y-0.5)^2}{b^2} + 1 > 0, \tag{57}$$

where we set $a = 0.45$ and $b = 0.2$ in our experiment. Fig. 8 shows the result of the subdivision of this ellipse after some steps of refinement. In each cell, the trimming function was approximated by a linear function as described in Section 4. Note that in the pentagonal case we integrate over the remaining triangle and subtract from the full integral. In the left plot in Fig. 9 we show the approximation error

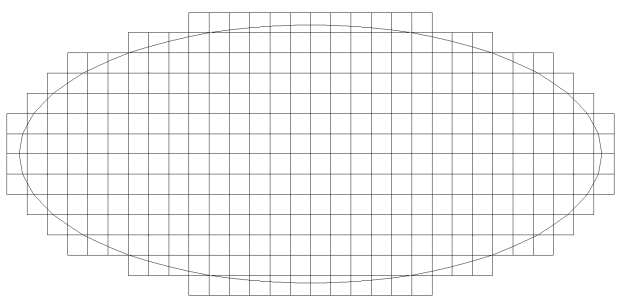

Fig. 8 Subdivision of the ellipse after some steps of refinement with approximate linear trimming curve in each cell.

for different values of h when computing the area enclosed by the ellipse with the simple trimmed quadrature $LT(h,1)$ described in Section 4 and with the trimmed quadrature by first order correction $CLT(h,1,2)$ described in Section 5. We observe that the first order error correction results in an additional order of convergence with respect to h, confirming the theoretical result from Theorem 1.

Next, we show the computation times for both quadrature rules in Fig. 10. We observe that applying the error correction does not result in a significant increase in complexity compared to the linearized trimmed quadrature. The complexity for both LT and CLT increases linearly with the number of cells.

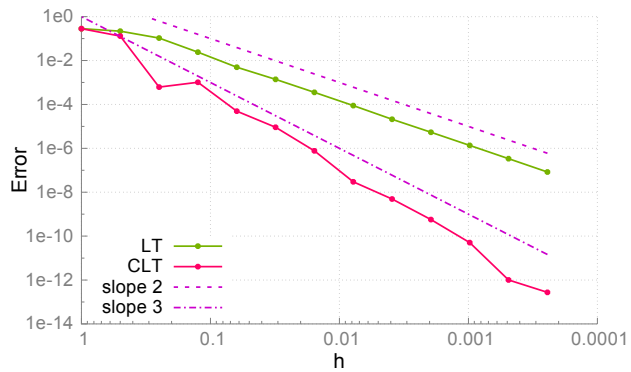

Fig. 9 Absolute error in LT and CLT for the area enclosed by the ellipse.

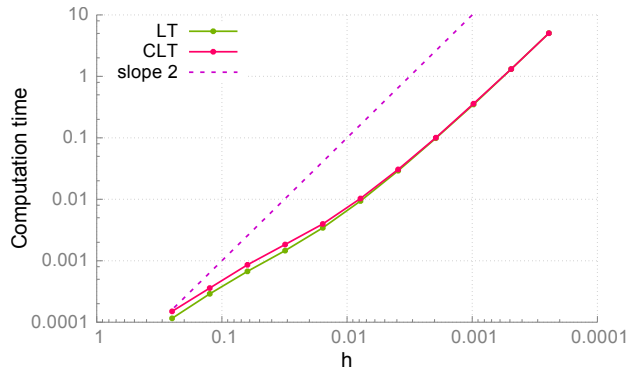

Fig. 10 Computation times for the approximation of the area enclosed by the ellipse

7.2 Perforated quarter annulus

In our next example, we will approximate the area of a quarter annulus which is trimmed with three circles. The quarter annulus is represented exactly as a NURBS domain. Fig. 11 shows the piece-wise linear approximation of the trimming curve in the computational and in the parametric domain after some steps of refinement. Since we perform the computation on the parametric domain, we approximate the integral

$$\int_{\Omega_{\gamma\circ G}} |\det J_G(x,y)| \mathrm{d}y\mathrm{d}x, \tag{58}$$

where $G : [0.1]^2 \to \mathbb{R}^2$ is the NURBS parameterization of the quarter annulus. The trimming function $\gamma : \mathbb{R}^2 \to \mathbb{R}$ on the physical domain is defined as the product of the implicit representations of the three circles.

In the first plot in Fig. 12 we show the convergence rate of the quadrature rules with and without error correction. We chose $n = 2$ Gauss nodes for the linearized

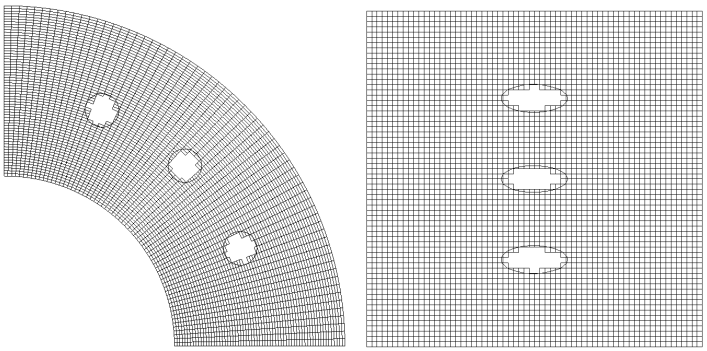

Fig. 11 Subdivision of the perforated quarter annulus and its corresponding parametric domain after some steps of refinement with approximate linear trimming curve in each cell.

quadrature and $k = 2$ Gauss nodes for the correction term. As in the case of the

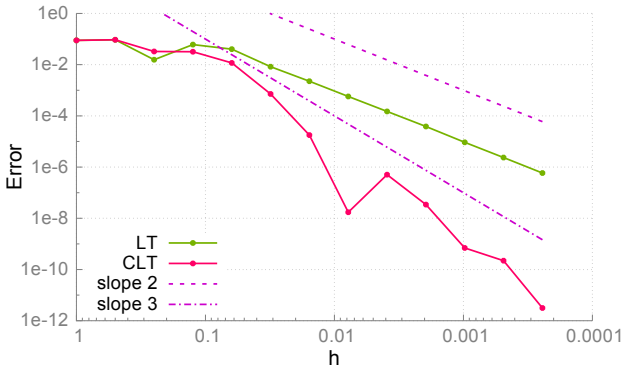

Fig. 12 Absolute error in LT and CLT for the area of the perforated quarter annulus for $n = 2, k = 2$.

ellipse, we observe that the first order error correction term in CLT results in an additional order of convergence compared to the linearized quadrature in LT.

Since we only use one error correction term, the convergence error cannot be improved by additional Gauss nodes in the bivariate and univariate quadrature. This is confirmed by the second plot in Fig. 13 which shows the same experiment as in the first plot but for $n = 3$ and $k = 3$.

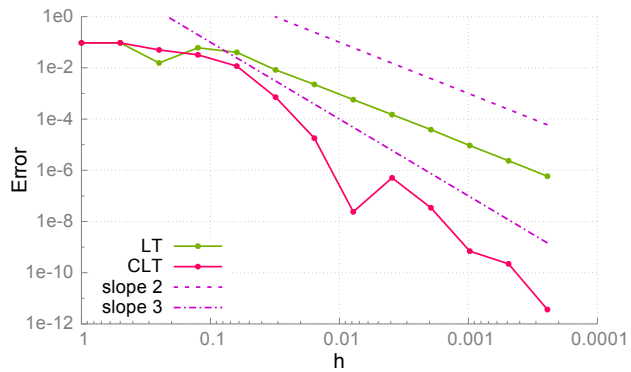

Fig. 13 Absolute error in LT and CLT for the area of the perforated quarter annulus for $n = 3, k = 3$.

7.3 Singular case: Bicuspid curve

Fig. 14 shows a linear approximation of the bicuspid curve which is an algebraic curve given by

$$(x^2 - a^2)(x - a)^2 + (y^2 - a^2)^2 = 0 \tag{59}$$

for some $a > 0$. It has two cusps that hinder the improvement of the approximation order by the error correction term. In Fig. 15 we show the error convergence of the

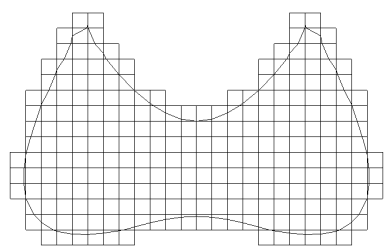

Fig. 14 Subdivision of the bicuspid with approximate linear trimming curve in each cell.

approximation of the area enclosed by the bicuspid, where the reference value was computed with a lower value of h. We observe that the error correction in CLT does not improve the convergence rate in this case, however, the absolute error is lower.

Acknowledgements The authors gratefully acknowledge the support provided by the Austrian Science Fund (FWF) through project NFN S11708 and by the European Research Council (ERC), project GA 694515.

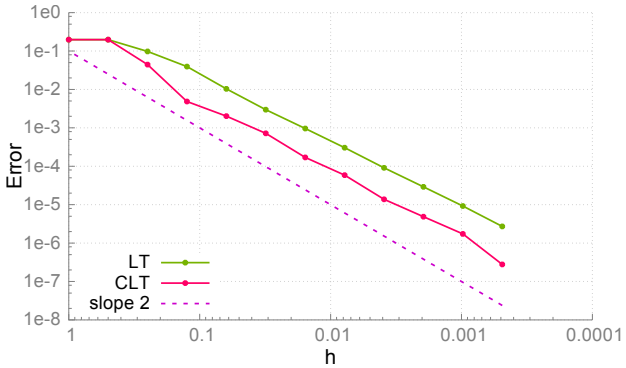

Fig. 15 Absolute error for the computation of the area enclosed by the bicuspid curve using LT and CLT.

References

1. Bandara, K., Rberg, T., Cirak, F.: Shape optimisation with multiresolution subdivision surfaces and immersed finite elements. Computer Methods in Applied Mechanics and Engineering **300**(Supplement C), 510 – 539 (2016)
2. Bazilevs, Y., Calo, V., Cottrell, J., Evans, J., Hughes, T., Lipton, S., Scott, M., Sederberg, T.: Isogeometric analysis using T-splines. Computer Methods in Applied Mechanics and Engineering **199**(5), 229 – 263 (2010)
3. Beer, G., Marussig, B., Zechner, J.: A simple approach to the numerical simulation with trimmed CAD surfaces. Computer Methods in Applied Mechanics and Engineering **285**, 776–790 (2015)
4. Cox, D.A., Sederberg, T.W., Chen, F.: The moving line ideal basis of planar rational curves. Computer Aided Geometric Design **15**(8), 803 – 827 (1998)
5. Gander, W., Gautschi, W.: Adaptive quadrature—revisited. BIT Numerical Mathematics **40**(1), 84–101 (2000)
6. Hofer, C., Langer, U., Toulopoulos, I.: Discontinuous Galerkin isogeometric analysis of elliptic diffusion problems on segmentations with gaps. SIAM Journal on Scientific Computing **38**(6), A3430–A3460 (2016)
7. Hofer, C., Toulopoulos, I.: Discontinuous Galerkin isogeometric analysis for parametrizations with overlapping regions. RICAM-Report **2017-17** (2017)
8. Hughes, T., Cottrell, J., Bazilevs, Y.: Isogeometric analysis: CAD, finite elements, NURBS, exact geometry and mesh refinement. Computer Methods in Applied Mechanics and Engineering **194**(39–41), 4135–4195 (2005)
9. Jüttler, B., Mantzaflaris, A., Perl, R., Rumpf, M.: On numerical integration in isogeometric subdivision methods for PDEs on surfaces. Computer Methods in Applied Mechanics and Engineering **302**, 131 – 146 (2016)
10. Kamensky, D., Hsu, M.C., Schillinger, D., Evans, J.A., Aggarwal, A., Bazilevs, Y., Sacks, M.S., Hughes, T.J.: An immersogeometric variational framework for fluid-structure interaction: Application to bioprosthetic heart valves. Computer Methods in Applied Mechanics and Engineering **284**, 1005 – 1053 (2015). Isogeometric Analysis Special Issue
11. Kim, H., Seo, Y., Youn, S..: Isogeometric analysis for trimmed CAD surfaces. Computer Methods in Applied Mechanics and Engineering **198**(37-40), 2982–2995 (2009)
12. Kumar, S., Manocha, D.: Efficient rendering of trimmed nurbs surfaces. Computer-Aided Design **27**(7), 509 – 521 (1995). Display and visualisation

13. Mantzaflaris, A., Scholz, F., others (see website): G+Smo (Geometry plus Simulation modules) v0.8.1. http://gs.jku.at/gismo (2018)
14. Marussig, B., Hiemstra, R., Hughes, T.: Improved conditioning of isogeometric analysis matrices for trimmed geometries. Computer Methods in Applied Mechanics and Engineering **334**, 79–110 (2018)
15. Marussig, B., Hughes, T.: A review of trimming in isogeometric analysis: Challenges, data exchange and simulation aspects. Archives of Computational Methods in Engineering pp. 1–69 (2017)
16. Nagy, A., Benson, D.: On the numerical integration of trimmed isogeometric elements. Computer Methods in Applied Mechanics and Engineering **284**, 165–185 (2015)
17. Newman, T.S., Yi, H.: A survey of the marching cubes algorithm. Computers & Graphics **30**(5), 854 – 879 (2006)
18. Rüberg, T., Cirak, F.: A fixed-grid b-spline finite element technique for fluid-structure interaction. International Journal for Numerical Methods in Fluids **74**(9), 623–660 (2014)
19. Ruess, M., Schillinger, D., Özcan, A., Rank, E.: Weak coupling for isogeometric analysis of non-matching and trimmed multi-patch geometries. Computer Methods in Applied Mechanics and Engineering **269**, 46–71 (2014)
20. Sanches, R., Bornemann, P., Cirak, F.: Immersed b-spline (i-spline) finite element method for geometrically complex domains. Computer Methods in Applied Mechanics and Engineering **200**(13), 1432 – 1445 (2011)
21. Schmidt, R., Wüchner, R., Bletzinger, K.U.: Isogeometric analysis of trimmed NURBS geometries. Computer Methods in Applied Mechanics and Engineering **241-244**, 93–111 (2012)
22. Scholz, F., Mantzaflaris, A., Jüttler, B.: Partial tensor decomposition for decoupling isogeometric Galerkin discretizations. Computer Methods in Applied Mechanics and Engineering **336**, 485 – 506 (2018)
23. Seiler, A., Jüttler, B.: Reparameterization and adaptive quadrature for the isogeometric discontinuous Galerkin method. In: Mathematical Methods for Curves and Surfaces, pp. 251–269. Springer International Publishing, Cham (2017)
24. Seo, Y.D., Kim, H.J., Youn, S.K.: Isogeometric topology optimization using trimmed spline surfaces. Computer Methods in Applied Mechanics and Engineering **199**(49-52), 3270–3296 (2010)
25. Taubin, G.: Estimation of planar curves, surfaces, and nonplanar space curves defined by implicit equations with applications to edge and range image segmentation. IEEE Transactions on Pattern Analysis and Machine Intelligence **13**(11), 1115–1138 (1991)
26. Zhang, H., Mo, R., Wan, N.: An IGA discontinuous Galerkin method on the union of overlapped patches. Computer Methods in Applied Mechanics and Engineering **326**, 446–480 (2017)
27. Zhu, X., Ma, Z., Hu, P.: Nonconforming isogeometric analysis for trimmed CAD geometries using finite-element tearing and interconnecting algorithm. Proceedings of the Institution of Mechanical Engineers, Part C: Journal of Mechanical Engineering Science **231**(8), 1371–1389 (2017)